

# The pulse shape and the spectrum of PSR B0531+21 (Crab pulsar) in the low-energy $\gamma$ rays observed with FIGARO II

E. Massaro<sup>1</sup>, M. Feroci<sup>2</sup>, E. Costa<sup>2</sup>, G. Matt<sup>3</sup>, B. Agrinier<sup>4</sup>, C. Gouiffes<sup>4</sup>, B. Parlier<sup>4</sup>, J.L. Masnou<sup>5</sup>, G. Cusumano<sup>6</sup>, T. Mineo<sup>6</sup>, B. Sacco<sup>6</sup>, L. Scarsi<sup>6</sup>, G. Gerardi<sup>7</sup>, M. Salvati<sup>8</sup>, P. Mandrou<sup>9</sup>, M. Niel<sup>9</sup>, and J.F. Olive<sup>9</sup>

<sup>1</sup> Istituto Astronomico, Università di Roma "La Sapienza", Unità GIFCO-CNR, via G.M. Lancisi 29, I-00161 Roma, Italy

<sup>2</sup> IAS, CNR, Roma, Italy

<sup>3</sup> Dipartimento di Fisica, Università di Roma Tre, Roma, Italy

<sup>4</sup> CEA,DSM/DAPNIA/Service d'Astrophysique, CEN-Saclay, France

<sup>5</sup> Université de Bordeaux, France

<sup>6</sup> IFCAI, CNR, Palermo, Italy

<sup>7</sup> Istituto di Fisica, Università di Palermo, Palermo, Italy

<sup>8</sup> Osservatorio Astrofisico di Arcetri, Firenze, Italy

<sup>9</sup> CESR, Université P. Sabatier, Toulouse, France

Received 11 December 1997 / Accepted 15 June 1998

**Abstract.** The FIGARO II experiment observed the Crab pulsar in the energy range 0.15–4 MeV during two transmediterranean flights, on 1990 July 9 and on 1986 July 11. A detailed analysis of the pulse profiles shows that the profile in the energy band 0.37–0.51 MeV is characterized, in addition to the main ones, by the presence in the Interpeak region of two other peaks, which could be associated with the 0.44 MeV line reported by Massaro et al. (1991). Spectral analysis confirms that the Ip spectrum, harder than those of P1 and P2, should progressively steepen with increasing energy. We conclude that the observed Crab emission can be due to the superposition of two components and that the one dominant in the Ip is associated with the pair production in the magnetosphere.

**Key words:** pulsars: individual: Crab pulsar (PSR B0531+21) –  $\gamma$ -rays: observations

## 1. Introduction

The study of the pulse profiles of spin powered pulsars is important to understand the mechanism and the site of particle acceleration. The Crab pulsar (PSR B0531+21), the only one detected over the full electromagnetic spectrum, is characterized by a double peak structure changing with the photon energy. The large area FIGARO II balloon borne experiment (Agnetta et al. 1989) observed this source in two flights in 1986 and 1990 and provided pulse profiles at energies greater than 0.3 MeV which are among the best ever obtained. Some results of these observations have already been presented in several papers (Agrinier et al. 1990; Massaro et al. 1991; Masnou et al. 1994). In particular, Massaro et al. (1991) reported the detection of a weak feature in the spectrum of the second peak at en-

ergy  $0.44 \pm 0.01$  MeV with intensity  $(0.86 \pm 0.33) 10^{-4}$  photons  $\text{cm}^{-2} \text{s}^{-1}$ . This was interpreted as  $e^+e^-$  annihilation radiation, redshifted by the intense gravitational field of the neutron star. In a first model developed by Bednarek et al. (1992) the annihilation line is produced by positrons interacting with the neutron star surface; more recently, Zhu & Ruderman (1997) have proposed a different model in which this line can be originated in an electron-positron layer, sustained above the neutron star surface by the radiation pressure of X rays enhanced by cyclotron resonant scattering.

In a couple of short contributions (Massaro et al. 1992, Olive et al. 1993) we presented some indication that the pulse shape in the energy band centred around 0.44 MeV is characterized by a complex structure. These preliminary analyses used only the 1990 flight data. In this paper, we present new results of a much more complete analysis of both observations confirming such anomalous structure. Moreover, we report the results of the phase spectroscopy of the 1990 flight in comparison with recent results of other experiments. Sect. 2 gives a brief description of the experiment and of the flight parameters; Sect. 3 summarizes the data reduction methods; in Sect. 4 the results of an analysis of the pulse shape, particularly in the region between the two main peaks, are presented; in Sect. 5 we discuss the dependence of the spectral slope on the phase and, finally, in Sect. 6 some implications of the present results for the emission model of PSR B0531+21 are discussed.

## 2. The FIGARO II experiment and balloon flights

The FIGARO II (French Italian GAMMA Ray Observatory) experiment was specifically designed to study the cosmic sources with a well established time signature in the low energy  $\gamma$  ray range. A detailed description of the experiment, calibration and performances is given by Agnetta et al. (1989). The detector is a square array of nine NaI(Tl) tiles with a geometric area of

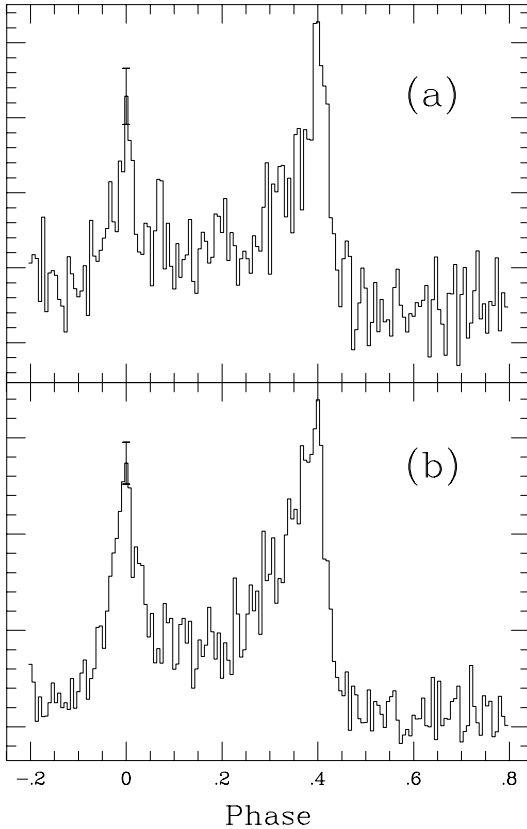


**Fig. 1a and b.** The pulse profiles of PSR B0531+21 observed with FIGARO II on 1986 July 11 (0.18-3.75 MeV) (a) and on 1990 July 9 (0.14-3.75) (b).

3600 cm<sup>2</sup>, actively shielded against cosmic ray and  $\gamma$ -ray background. Downwards charged particles are anticoincided by a thin plastic scintillator on the top of the whole detector. The energy ranges were (0.18-6) MeV in 1986 and (0.14-4.2) MeV in 1990, respectively. The latter choice allowed a narrower energy binning (0.018 MeV instead of 0.027 MeV per bin of the previous flight). The time and energy channel of each individual accepted trigger were transmitted one by one at a ground station with a bit rate of 300kHz bandwidth. Only in the case of the second (1990) flight, data were also registered on.

FIGARO II was first launched from the Milo base (Trapani, Italy) on 1986 July 11. The Crab observation, started during the final part of the ascent, was stopped after about 2.3 hours at ceiling for a total duration of 8220 s. The second flight was on 1990 July 9, again from Milo, and the Crab tracking started at 7:06 UT at a residual pressure of 9 mbar. The ceiling (4.4 mbar) was reached 36 minutes later and remained stable for the entire observation time (20,900 s). The effective accuracy of the timing, including the numerization of the analogic data, is approximately 30  $\mu$ s under standard conditions; the details are described in Masnou et al. (1994).

### 3. Data analysis

The arrival time of each event was transformed into the solar system barycentre using the Jet Propulsion Laboratory Ephemeris

Code DE200 (Standish, 1982) and the precession corrected coordinates of the Crab pulsar (Lyne & Pritchard 1993, see Masnou et al. 1994 for details). The pulsed light-curve of PSR B0531+21 was computed by folding the arrival time of each accepted event with the instantaneous period extrapolated from radio data. The phases  $\phi(t)$  of single photons were computed according to the formula:

$$\phi(t) = \nu(t - t_0) + \frac{1}{2}\nu'(t - t_0)^2 \quad (1)$$

where  $t_0$  is the reference epoch. The pulsar parameters at  $t_0$  were derived from the Jodrell Bank Crab Pulsar Monthly Ephemeris (Lyne & Pritchard, 1993) for nearly contemporary radio measurements, respectively 1986 July 15 and 1990 July 15. For the 1986 observation, the adopted values of the frequency and frequency derivative were  $\nu = 30.0063102270$  Hz and  $\nu' = -3.7931791 \times 10^{-10} \text{ s}^{-2}$  at the reference epoch  $t_0 = 2,446,626.5$  JD; for 1990 we used  $\nu = 29.9585217157$  Hz and  $\nu' = -3.7793430 \times 10^{-10} \text{ s}^{-2}$  at  $t_0 = 2,448,087.5$  JD. The resulting phase histograms for the 1986 and 1990 flights are shown in Figs. 1a and 1b, respectively; the zero phase has been taken at the centre of the first peak (P1).

The evaluation of the pulsed intensity and spectrum depends on the background which must be subtracted from the total signal. PSR B0531+21 is embedded in a nebular remnant, which is very bright in X and  $\gamma$  rays, and therefore a simple measurement of the background count rate in an offset direction is not sufficient. The usual approach is to establish an off-pulse phase interval where to compute the average background. The statistical noise of all known low energy  $\gamma$ -ray data does not allow a good enough definition of this phase interval. We, therefore, considered observations at lower energies (Harnden & Seward 1984, Mineo et al. 1997) which show a quite extended trailing edge of the second peak (P2) and adopted 0.55-0.8 as best choice for the off-pulse interval. Following Agrinier et al. (1990) we used the intervals (-0.05-0.05), (0.05-0.27), and (0.27-0.47) for P1, Ip, and P2, respectively.

## 4. The pulse shape in the low-energy gamma rays

### 4.1. Overall shape of pulse profiles

As we said above the pulse profiles are dominated by the two peak structure, characterized, in this energy range, by the prominence of P2. A few differences between the two observations, however, are apparent: the width of P1 in the 1986 profile is narrower than in 1990, suggesting a possible variability, and the emission bridge between the peaks (the Interpeak Region - Ip) seems to be particularly structured in the former flight.

In the panels of Fig. 2, the phase histograms in five energy ranges for both the observations are shown. The two peak structure is easily recognizable in all the profiles with the exception of the highest energy one of the 1986 flight (Fig. 2e). While in the low energy intervals the pulse profiles are rather smooth, possible features, between the two major peaks, appear in the energy range (0.37-0.51) (Fig. 2c,c'). The most prominent one is present in the 1986 data at the phase 0.3, suggesting a double

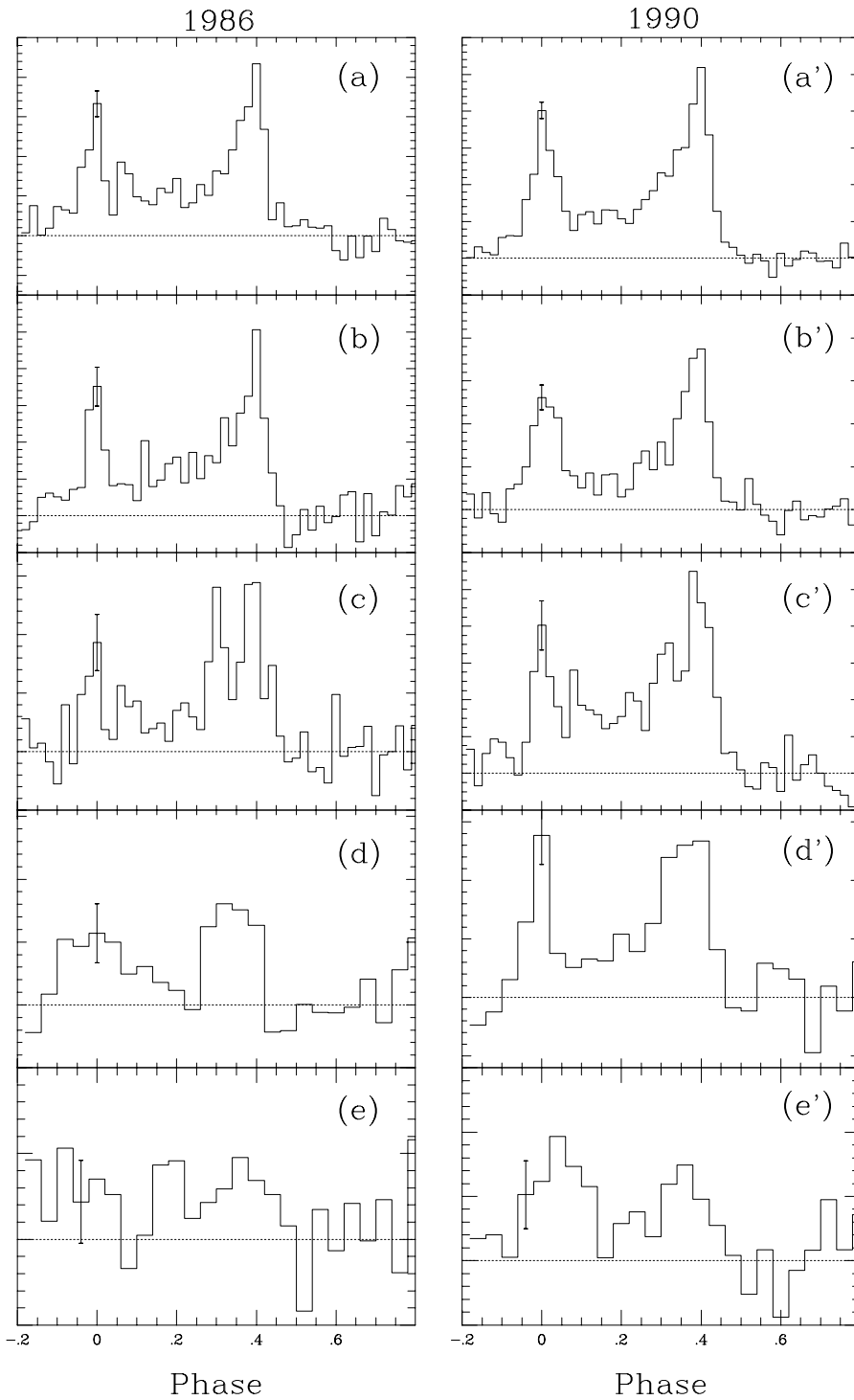


**Fig. 2a–e’.** The pulse profiles of PSR B0531+21 for the 1986 and 1990 flights in five similar nominal energy ranges: 0.18–0.26 (a), 0.15–0.26 (a’), 0.26–0.37 (b,b’), 0.37–0.51 (c,c’), 0.51–1.05 (d,d’) and 1.05–3.72 (e,e’) MeV. The dotted lines indicate the off-pulse level.

structure of P2. A possible feature at the same phase may also be present in the corresponding profile of the 1990 observation, but less evident. Furthermore, in the same curves another structure could be present in Ip region at the phase 0.08.

Because these phase histograms do not have a S/N ratio comparable with those at lower energies and the fluctuations could produce the impression of spurious features, we computed some smoothed profiles. They were obtained by means of the Kernel

Density Estimator algorithm (De Jager et al. 1986), already used in the study of pulsar signals. We worked on 300 bin profiles and used a gaussian kernel with a  $\sigma$  equal to 3.5 bin, which, after a few trials, was estimated to be a good compromise between the smoothing efficiency and resolution. This method allows to evaluate the standard deviation for the smoothed content of each individual bin, providing a further tool to evaluate the statistical significance of the features. The resulting phase histograms,

for the two flights confirm the relevance of the peak at 0.3 in the 1986 data with a total intensity comparable with that of the other peaks and much higher than the typical noise fluctuations (Lemoine 1992). Other emerging possible features are the one close to 0.1 in the 1990 data and in the same energy range, and another in the 1986 data at the lowest energies again at 0.1. To be more confident of their statistical significance we performed some further tests which are described in the following section.

#### 4.2. The shape of the interpeak region and the significance of the minor peaks

The pulse shape of PSR B0531+21 is poorly known above 0.3 MeV and a well established profile to be used as a template is not available. In order to evaluate the statistical significance of the extra structures present in the 0.37-0.51 MeV range we had, therefore, to compare these data with those at different energies. We decided to normalise to unity the total content of the phase histograms within the interval (-0.05-0.47), after subtraction of a constant level, defined as the mean value of the off-pulse interval.

In the analysis of the 1986 observation, when the feature at the phase 0.3 was more prominent, we used the low energy (0.18-0.37 MeV) profile of the same observation as a template. The phase histograms for the two bands are compared in Fig. 3a. The differences of the three bins of phase containing the feature with respect to the low energy ones are 1.36, 3.23, 0.75 standard deviations, taking into account the statistical errors on both curves; the resulting total significance (estimated adding the three previous values in quadrature) is 3.58 standard deviations. This normalisation reduces the difference between the content of the feature bins in the two histograms, because the feature itself contributes to the integral value; this is indeed evident from the other bins, which are systematically lower in the high energy histogram with respect to the other one. Limiting the normalisation to the (-0.05-0.25) phase interval, (Fig. 3b), we found that the differences increase to 1.81, 3.93 and 1.46 standard deviations respectively, and the significance of the whole structure to 4.57  $\sigma$ . We can, therefore, conclude that the probability that such an effect was produced by a chance fluctuation is really marginal and it must be considered real.

A similar analysis performed on the data of the 1990 flight does not give a comparable evidence for the suspected features (Fig. 4). We see, however, that in the (0.37-0.51) MeV histogram the content of the two bins at the phase 0.3 is higher than those at lower energies, while the content of the two following bins is smaller, suggesting again the presence of a feature. These differences are 0.75, 1.79, 1.38 and 1.65 standard deviations, which added in quadrature give the combined significance of 2.90  $\sigma$ . Of course, this computation is justified only by the previous result found the 1986 data, but it is worthwhile that it provides a further indication in the direction of the former finding. Notice also in Fig. 4 the difference in the trailing edge of P1, which is narrower in the (0.37-0.51) MeV band, and the excess at the phase 0.08 corresponding to 1.92 standard deviations.

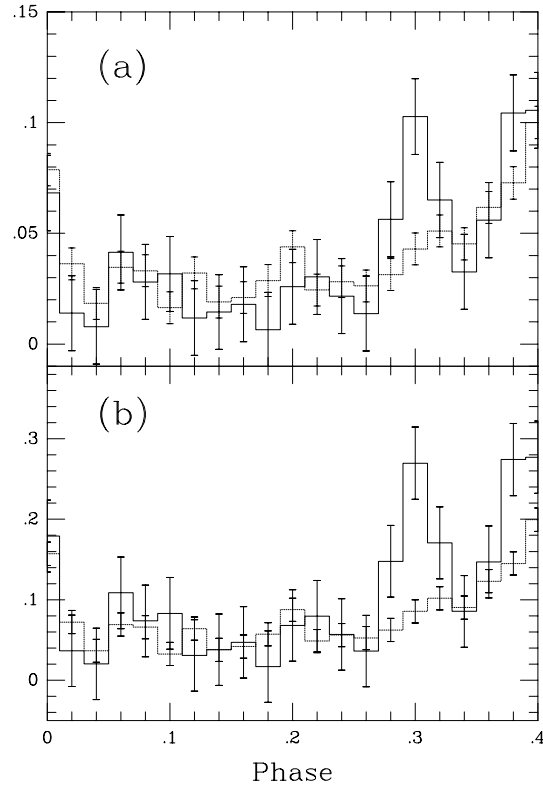


**Fig. 3a and b.** Comparison between the interpeak regions observed in 1986 flight in two different energy ranges: 0.18-0.37 MeV (dotted line) and 0.37-0.51 MeV (solid line). Data of panel a were normalised to unity in the phase interval (-0.05-0.47) and those of panel b in the interval (-0.05-0.25) to exclude the feature at 0.3.

We studied also the shape of the Ip region using a different approach. The profile segment between the maxima of P1 and P2, corresponding to the phase interval (0.0-0.4) was modeled by means of an analytical formula whose parameters were determined by a  $\chi^2$  minimisation. We adopted a sum of two power laws which gave acceptable fits of the low energy data, 0.18-0.37 MeV, of the two flights summed together. It can be written as

$$F(\phi) = \frac{A}{|\phi - \phi_1|^m} + \frac{B}{|\phi - \phi_2|^n} \quad (2)$$

The fitting results showed a high correlation between the parameters' values, and consequently We decided to fix two of them to their best fit values ( $m=25$  and  $n=1.5$ ). The best estimates of the remaining free parameters were  $A = 2.736 \times 10^{-2}$ ,  $B = 3.964 \times 10^{-3}$ ,  $\phi_1 = 0.9648$ , and  $\phi_2 = 0.5121$  with a reduced  $\chi^2$  of 1.09 (17 d.o.f). The data and the Eq. (2) curve are shown in Fig. 5a.

When this low energy best fit curve is applied to the (0.37-0.51 MeV) energy range for the sum of the two observations (Fig. 5b), the reduced  $\chi^2$  of 1.81 (21 d.o.f) and the corresponding probability of 0.015 are obtained. Again if Eq. (2) is fitted to the same data the reduced  $\chi^2$  lowers to 1.71 (17 d.o.f) corresponding to the probability of 0.035. These results provide

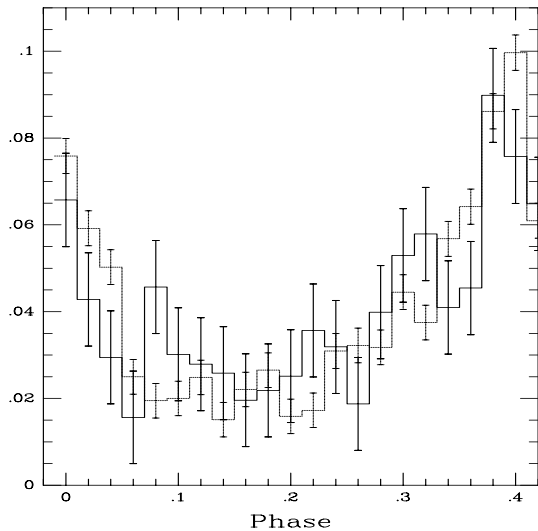


**Fig. 4.** Comparison between the interpeak regions observed in 1990 flight in two different energy ranges: 0.18-0.37 MeV (dotted line) and 0.37-0.51 MeV (solid line). The data were normalised to unity in the phase interval (-0.05-0.47).

**Table 1.** The P2/P1 and Ip/P1 ratios measured in the two FIGARO II flights.

Energy Range (MeV)	P2/P1(86)	P2/P1(90)	Ip/P1(86)	Ip/P1(90)
0.16-0.26	$2.28 \pm .22$	$2.05 \pm .10$	$1.38 \pm .16$	$0.99 \pm .07$
0.26-0.37	$2.34 \pm .34$	$1.85 \pm .15$	$1.29 \pm .24$	$0.82 \pm .11$
0.16-0.37	$2.31 \pm .17$	$1.94 \pm .07$	$1.34 \pm .13$	$0.98 \pm .05$
0.37-0.51	$3.56 \pm .89$	$2.59 \pm .37$	$1.41 \pm .47$	$1.52 \pm .26$
0.51-1.05	$2.25 \pm .77$	$2.18 \pm .48$	$0.90 \pm .50$	$0.96 \pm .33$
1.05-3.72		$1.32 \pm .46$		$1.34 \pm .48$

an additional indication, at a confidence level greater than 2 standard deviations, that the shape of the Ip region changes in the energy interval 0.37-0.51 MeV with respect to the lower energies, because of the apperancy on these additional features.

#### 4.3. The P2/P1 and Ip/P1 ratios

It is well known from a large number of past observations that the intensity ratio of the two main peaks P2/P1 increases from the soft X rays to about 1 MeV and goes down to quite small values above 30 MeV (see the database by Massaro et al. 1997a). A satisfactory explanation of this behaviour is still lacking: it is likely that it corresponds to the onset of an emission component peaked between 0.03 and 1.0 MeV, but its nature and location within the magnetosphere are far to be understood.

We evaluated the P2/P1 and Ip/P1 ratios for the phase intervals given in Sect. 3. These are slightly different from those used by Ulmer et al. (1994), who took for Ip and P2 (0.08-0.27) and (0.3-0.44). No general agreement exists among the various authors because the choice depends on the particular energy range and sensitivity of the experiments. Notice that with our choice the feature at 0.3 is entirely included within the P2 interval, whereas with the other only half of it would be considered.

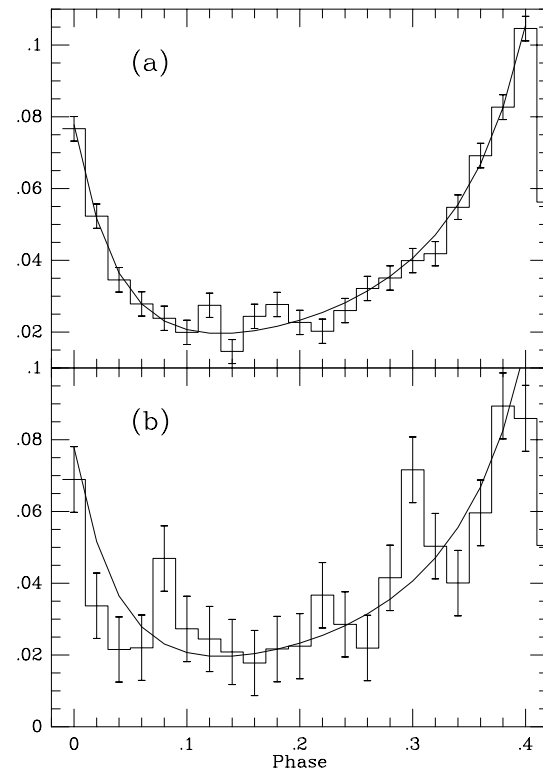


**Fig. 5a and b.** The interpeak regions observed in both flights summed together in the energy ranges 0.18-0.37 MeV (a) and 0.37-0.51 MeV (b). The solid line is the fitting curve of Eq. (2).

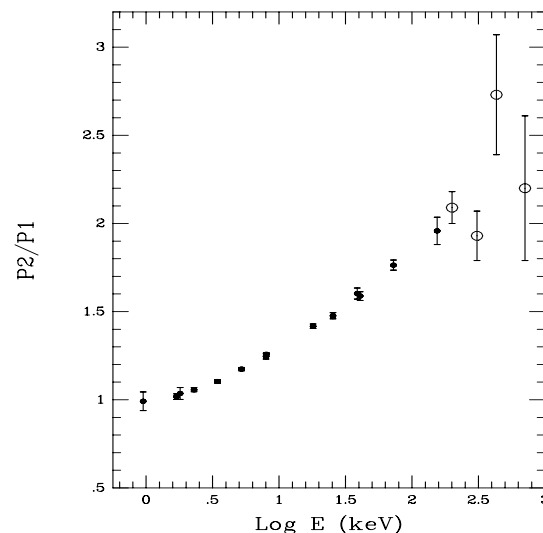


**Fig. 6.** The energy dependence of the P2/P1 ratio. Solid circles are the data of BeppoSAX 1996 observation (Mineo et al. 1997), the open circles are the means of the two FIGARO II flights.

In computing the statistical errors of these ratios one must take into account that the net fluxes of the two peaks are not statistically independent because of the subtraction of a common

**Table 2.** Comparison between the spectral indices measured with FIGARO II in the 1990 flight and those of other experiments.

Experiment	Energy Range (MeV)	P1	Ip	P2	Total
FIGARO II	0.15-0.5	2.27±.14	2.27±.21	2.12±.10	2.19±.10
GRIS	0.03-1.0	2.01±.06	2.05±.16	1.97±.06	2.04±.05
OSSE 1	0.06-0.5	2.07±.03	1.93±.05	2.00±.03	1.99±.03
OSSE 2	~0.10-0.5	2.35	2.16	2.41	2.25
CGRO 1	0.06-10 <sup>4</sup>	2.17±.001	2.24	2.18	2.16
CGRO 2	~0.15-10 <sup>4</sup>	2.09±.02	2.53±.23	2.55±.02	2.20±0.02
BeppoSAX(PDS)	0.02-0.3	2.02±.02	1.72±.05	1.88±.02	2.03±.005
RossiXTE	0.005-0.15	1.92±.005	1.69±.05	1.80±.005	

off-pulse level. The variance of the ratio  $\sigma_r$  thus includes a non-zero covariance term:

$$\sigma_r^2 = \left(\frac{F_2}{F_1}\right)^2 \left[ \frac{\sigma_2^2}{F_2^2} + \frac{\sigma_1^2}{F_1^2} - 2\frac{cov(F_1, F_2)}{F_1 F_2} \right] \quad (3)$$

where  $F_1$ ,  $\sigma_1$  and  $F_2$ ,  $\sigma_2$  are the fluxes and standard deviations of total signals in the considered phase intervals, respectively. Since the counts in each phase bin are statistically independent on those in the other bins, it is easy to show that

$$cov(F_1, F_2) = w_1 w_2 \sigma_{op}^2 \quad (4)$$

where  $w_1$  and  $w_2$  are the interval widths and  $\sigma_{op}^2$  is the single bin mean variance of the off-pulse counts.

The values of P2/P1 and Ip/P1 for the two flights in the same energy bands of Fig. 2 are given in Table 1: no significant variation within the experimental errors is appreciable between the two epochs. If the two lowest bands are summed together, only a marginal evidence of a decrease of P2/P1 and Ip/P1 at the level of two standard deviations can be appreciated. Such effect is essentially due to smaller values of P1 in 1986 (see Figs. 1 a,b), at variance with the energies greater than 50 MeV, where the changes are due to P2.

In Fig. 6 the average values of P2/P1 measured in the two flights are shown together with the very recent estimates obtained with the broad band Italian-Dutch satellite BeppoSAX (Mineo et al. 1997). Nevertheless the large uncertainties at high energies, these data indicate that the ratio increases up to MeV range, in agreement with the COMPTEL result (Carraminana et al. 1994).

## 5. Spectral analysis

The results of the phase resolved spectroscopy of the 1986 flight were already described by Agrinier et al. (1990). Here we report the analysis of the second observation, of which only the detection of the weak feature at 0.44 MeV was presented (Massaro et al. 1991). The spectra of the pulsed signals in selected phase intervals were computed from the net counts obtained by subtracting the mean off-pulse level and the spectral parameters were evaluated by means of the XSPEC code.

In Table 2 we report the values of the spectral index  $\alpha$  of the 1990 flight in the energy range 0.15-0.5 MeV. For comparison we have also listed in the same table the  $\alpha$  values measured with GRIS (Bartlett et al. 1994), OSSE (Ulmer et al. 1994), Compton-GRO, including COMPTEL and EGRET data (Ulmer et al. 1995), and also those recently obtained with the Phoswich Detector System PDS (Frontera et al. 1997) on board BeppoSAX (Cusumano et al. 1997a) and RossiXTE (Pravdo et al. 1997). Two estimates of the spectral index  $\alpha$ , for a single (1 in Table 2) or a double power law (2 in Table 2), are given for OSSE and Compton-GRO; in the latter case the reported values are those of the higher energy band which is more similar to the FIGARO range, being the break energy generally close to 0.1 MeV. We recall also that the phase intervals used in these two analyses are not exactly coincident with ours and this fact can produce some slight different  $\alpha$  values.

A good agreement, within the statistical uncertainties, exists between the FIGARO spectral indices and those of the two power law model for the OSSE data, whereas the greatest differences are with the BeppoSAX and RXTE values. These discrepancies can be explained by the different energy ranges. Notice that the spectrum of the Ip for these two experiments is quite harder than the others indicating a continuous steepening with increasing energy. This effect is further strengthened by the high  $\alpha$  values for Ip and P2 of the CGRO(2) spectra which include also GeV energies. The  $\alpha$  estimates of GRIS and OSSE (one power law) are practically the same for all the phase intervals. This agrees with the above picture if the spectral fits were statistically dominated by the data points between ~0.05 and 0.10 MeV. These spectral behaviour indicate the complexity of the Crab spectral distribution in the hard X rays and low energy  $\gamma$  rays. It is indeed possible that it is produced by the superposition of two components, likely located in different sites of the magnetosphere, as we will discuss in the next section.

## 6. Discussion

The main results of the present analysis indicate the presence of new significant features, in addition to the main peaks, in the pulse profile of PSR B0531+21. These features, clearly evident in the Ip region at the phases 0.08 and 0.3, are detectable only in a rather narrow energy band centered at about 0.44 MeV and therefore they are likely related to the weak spectral feature de-

scribed by Massaro et al. (1991). Moreover, they seem also to be variable, because the feature at 0.3, very prominent in the 1986 flight, is only marginally detectable in the 1990 data. Discoveries of spectral features, generally transient, were reported several times in the literature and have been summarized by Owens (1991).

Search for extra features was performed several times in the past, in particular in the hard X-ray range, but no firm conclusion about their existence was reached. We recall the early observations by Ducros et al. (1970), which found two minor features at the phases 0.13 and 0.55, and by Ryckman et al. (1977) which reported a transient structure at 0.65 in the energy band 35-116 keV. Agrinier et al. (1990) gave evidence of a minor feature at energies greater than 0.5 MeV at the phases  $\sim 0.8$  and 0.2, the former at same position of a possible excess already noted by Kurfess (1971) and of the spectral hardening observed by RXTE (Pravdo et al. 1997). Complex and structured radio profiles have been more recently reported by Moffet & Hankins (1996): in particular they found a small component at the phase  $\sim 0.9$  (1.4-4.9 GHz) and two more prominent and broad features (4.7-8.4 GHz) centred at 0.57 and 0.73 in the off pulse.

Only very few pulse profiles in the same energy range of the features found by us have been published in the literature. Wilson & Fishman (1983) report a phase histogram in the energy range (0.36-0.53) MeV much more noisy than ours and not useful for the search of minor structures. The OSSE (0.34-0.50) MeV profile (Ulmer et al. 1994) is also characterized by rather poor statistics and small features can hardly be detected. In any case, the Ip has a complex shape and cannot be fitted by Eq. (2).

Beside these narrow band features, we detect systematic trends in the dependence of the pulse profile with energy (P1/P2 ratio, spectral index in different phase intervals), which connect smoothly with the results of other experiments in adjacent bands. All these broad band trends can be explained with one single assumption, as already discussed in Mineo et al. (1997) and Massaro et al. (1998). They suggest that one additional component must be added to a template pulse profile; the latter is identified with that in the optical, and is independent of energy; the former is broader in phase, and appears at X-ray, low  $\gamma$ -ray energies with an intensity which parallels the curve of Fig. 6.

A physical basis for the origin of the narrow band feature, possibly associated with  $e^+e^-$  annihilation, and of the broad band additional component has been proposed by Zhu & Ruderman (1997) and Wang et al. (1998). The “blanket” of pairs, showering down the inner magnetosphere and piling up at very small radii, is expected to produce a synchrotron continuum and a redshifted annihilation line; it is worth pointing out that the redshift measured by Massaro et al. (1991) and the annihilation radius computed by Zhu & Ruderman (1997) imply a neutron star mass of 1.4-1.5  $M_{\odot}$ .

*Acknowledgements.* We are grateful to M. Ruderman for enlightening discussions on pulsar models and to L. Angelini for useful conversations on the recent observational results. The Palermo and Rome groups acknowledge the financial support from the ASI - Agenzia Spaziale Italiana.

## References

- Agnetta, G., Di Raffaele, R., Mineo, T. et al., 1989, Nucl. Instr. Meth. A 281, 197
- Agrinier, B., Masnou, J.L., Parlier, B. et al., 1990, ApJ 355, 645
- Bartlett, L.M., Barthelmy, S.D., Gehrels, N. et al., 1994, Proc. 3rd Compton Symp., AIP, p. 67
- Bednarek, W., Cremonesi, O., Treves, A., 1992, ApJ 390, 489
- Carraminana, A., Bennet, K., Buccheri, R. et al., 1994, A&A 290, 497
- Cusumano, G., Dal Fiume, D., Giarrusso, S. et al., 1997, Proc. 4th Compton Symp. (C.D. Dermer, M.K. Strickman and J.D. Kurfess eds.), AIP 410, 553
- DeJager, O.C., Raubenheimer, B.C., Swanepoel, J.W.H., 1986 A&A 170, 187
- Ducros, G., Ducros, R., Rocchia, R. et al., 1970, Nature 227, 152
- Frontera, F., Costa, E., Dal Fiume, D. et al., 1997, A&AS 122, 357
- Harnden, F.R., Seward, F.D., 1984, ApJ 283, 279
- Kurfess, J.D., 1971, ApJ 168, L39
- Lyne, A.G., Pritchard, R.S. 1993, Jodrell Bank Crab Pulsar Timing Results Monthly Ephem., Univ. of Manchester
- Lemoine, D., 1992, CEN Report
- Masnou, J.L., Agrinier, B., Barouch, E. et al., 1994, A&A 290, 503
- Massaro, E., Matt, G., Salvati, M. et al., 1991, ApJ 376, L11
- Massaro, E., Agrinier, B., Barouch, E. et al., 1992, Proc. Compton Observ. Sci. Workshop (C.R. Shrader, N. Geherel and B. Dennis eds.), NASA Conf. publ. 3137, p. 222
- Massaro, E., Feroci, M., Matt, G., 1997, A&AS 124, 123
- Massaro, E., Litterio, M., Cusumano, G. et al., 1998, Proc. “The Active X-ray Sky” (L. Scarsi, H. Bradt, P. Giommi & F. Fiore eds.) Nucl. Phys. B Conf., in the press
- Mineo, T. et al., 1997, A&A 327, L21
- Moffett, D.A., Hankins, T.H., 1996, ApJ 468, 779
- Olive, J.F., Agrinier, B., Barouch, E. et al., 1993, A&AS 97, 321
- Owens, A., 1991, in *Gamma-Ray Line Astrophysics*, eds. P. Durouchoux & N. Prantzos. (New York: AIP Conf. Proc. No. 232), p.341
- Pravdo, S.H., Angelini, L., Harding, A.K., 1997, ApJ 491, 808
- Ryckman, S.G., Ricker, G.R., Scheepmaker, A. et al., 1977, Nature Phys. Sci. 266, 431
- Standish, E.M., 1982, A&A 114, 297
- Ulmer, M.P., Lomatch, S., Matz, S.M. et al., 1994, ApJ 432, 228
- Ulmer, M.P., Matz, S.M., Grabelsky, D.A. et al., 1995, ApJ 448, 356
- Wang, F.Y.-H., Ruderman, M., Halpern, J.P., Zhu, T., 1998 ApJ 498, 373
- Wilson, R.B., Fishman, G.J., 1983, ApJ 269, 273
- Zhu, T., Ruderman, M., 1997, ApJ 478, 701